

A CLASS OF IMPLICIT-EXPLICIT TWO-STEP RUNGE-KUTTA METHODS *

EVGENIY ZHAROVSKY[†] AND ADRIAN SANDU[‡]

Abstract. This work develops implicit-explicit time integrators based on two-step Runge-Kutta methods. The class of schemes of interest is characterized by linear invariant preservation and high stage orders. Theoretical consistency and stability analyses are performed to reveal the properties of these methods. The new framework offers extreme flexibility in the construction of partitioned integrators, since no coupling conditions are necessary. Moreover, the methods are not plagued by severe order reduction, due to their high stage orders. Two practical schemes of orders four and six are constructed, and are used to solve several test problems. Numerical results confirm the theoretical findings.

Keywords: Implicit-explicit methods, two step Runge Kutta, order reduction

1. Introduction. Many science and engineering problems require numerical simulations of multiphysics systems, i.e., systems driven by multiple simultaneous physical processes evolving at different time scales. Processes can be categorized according to their characteristic time scales into fast (stiff) and slow (non-stiff).

In this work are concerned with solving the following system of ordinary differential equations (ODEs)

$$y'(t) = f(y) + g(y), \quad t_0 \leq t \leq t_F, \quad y(t_0) = y_0; \quad y(t) \in \mathbb{R}^N, \quad (1.1)$$

where f and g represent the non-stiff and the stiff processes, respectively. Without loss of generality, we skip the explicit dependence of f and g on the time argument. Problems of the form (1.1) often arise from the spatial discretization of partial differential equations (PDEs) in the method of lines approach; in this case y is the semi-discrete state. As an example consider advection-diffusion-reaction systems where the advection is slow while the diffusion and chemistry are typically fast [10, 26, 35]. Another example is the semi-implicit time integration of PDEs, where g represents the linear part of the discretized spatial operator, and f is its nonlinear part [8, 11, 24].

The best numerical solution strategy for a particular problem depends on its dynamics. For non-stiff processes explicit time discretizations are the most efficient, due to their low cost per step. For stiff processes explicit methods require prohibitively small time steps (limited by the fastest time scale in the system). In this case implicit methods are more efficient as their step sizes are not limited by stability considerations [13, 14]. The numerical solution of multiphysics systems (1.1) is challenging as neither purely explicit nor purely implicit methods are completely satisfactory. Explicit methods have restricted time steps (due to g), while implicit methods require the solution of (non)linear systems of equations that involve *all* the processes in the model.

The implicit-explicit (IMEX) approach alleviates these difficulties by combining an implicit scheme for the stiff component with an explicit scheme for the non-stiff component. The pair is chosen such that the overall discretization of (1.1) has the

*Adrian Sandu was supported by the National Science Foundation through awards NSF CCF-0916493, NSF OCI-0904397, NSF DMS0915047, and NSF CCF-0515170. Evgeniy Zharovsky was supported by the TUM IGSSE project 3.02

[†]Chair of Numerics, Technische Universität München, Boltzmannstr. 3 D-85748 Garching, Germany. E-mail: evgeniy.zharovsky@gmail.com

[‡]Computational Science Laboratory, Department of Computer Science, Virginia Tech, 2200 Kraft Drive, Blacksburg, VA 24061, USA. E-mail: sandu@cs.vt.edu.

desired stability and accuracy properties. IMEX linear multistep (LM) methods have been proposed in [9, 16, 32] and IMEX Runge-Kutta (RK) schemes in [33, 2, 21, 34]. The orders of consistency of these methods is typically lower than five. High order IMEX RK methods are difficult to construct due to the large number of order conditions. IMEX LM methods have decreasing stability properties with increasing order.

General linear (GL) methods [3, 4, 7, 15, 28] represent a natural generalization of both RK and LM methods, as they use both internal stages and information from previous solution steps. Two step Runge Kutta (TSRK) methods are a subclass of general linear methods that uses the stage values from only one previous step [1, 18, 23, 29]. The added flexibility of GL methods allows to design algorithms with superior stability and accuracy properties. However, to the best of our knowledge, the GL framework has not been previously employed to construct IMEX methods.

This work proposes a new family of implicit-explicit methods based on pairs of TSRK schemes. The order conditions and the stability properties of the resulting discretization are investigated. Two practical IMEX TSRK methods are constructed, and are used in numerical tests to illustrate the theoretical findings.

The remainder of the paper is organized as follows. Section 2 introduces the partitioned two-step Runge Kutta methods, and order conditions are derived in Section 2.3. Implicit-explicit TSRK methods are proposed in Section 3, and their stability properties are discussed in Section 4. Practical IMEX TRSK methods are constructed in Section 5, and are used in numerical tests in Section 6. Conclusions are drawn in Section 7.

2. Partitioned two-step Runge Kutta methods.

2.1. Two-step Runge Kutta (TSRK) methods. Consider the system of ordinary differential equations (ODEs)

$$y' = f(y), \quad y(t_0) = y_0, \quad t_0 \leq t \leq t_F. \quad (2.1)$$

A TSRK method advances (2.1) from t_n to $t_{n+1} = t_n + h$ as follows [17]:

$$Y_i^{[n]} = (1 - \mathbf{u}_i) y_{n-1} + \mathbf{u}_i y_{n-2} + h \sum_{j=1}^s \left(a_{i,j} f(Y_j^{[n]}) + b_{i,j} f(Y_j^{[n-1]}) \right), \quad i = 1, \dots, s, \quad (2.2a)$$

$$y_n = (1 - \vartheta) y_{n-1} + \vartheta y_{n-2} + h \sum_{j=1}^s \left(v_j f(Y_j^{[n]}) + w_j f(Y_j^{[n-1]}) \right). \quad (2.2b)$$

The method (2.2) can be represented compactly by its tableau of coefficients [17]

$$\begin{array}{c|cc} \mathbf{u} & \mathbf{A} & \mathbf{B} \\ \hline \vartheta & \mathbf{v}^T & \mathbf{w}^T \end{array}, \quad (2.3)$$

where $\mathbf{A} = (a_{i,j})_{1 \leq i,j \leq s}$, $\mathbf{B} = (b_{i,j})_{1 \leq i,j \leq s}$, $\mathbf{u} = (u_i)_{1 \leq i \leq s}$, $\mathbf{v} = (v_i)_{1 \leq i \leq s}$, $\mathbf{w} = (w_i)_{1 \leq i \leq s}$, and ϑ is a scalar. In addition the abscissa vector $\mathbf{c} = (c_i)_{1 \leq i \leq s}$ describes the time points where stage approximations are computed.

The TSRK method (2.2) has *stage order* q [18] if the stage vectors $Y_j^{[n]}$ are order q approximations of the exact solution at $t_{n-1} + c_j h$

$$Y_j^{[n]} = y(t_{n-1} + c_j h) + \mathcal{O}(h^{q+1}), \quad h \rightarrow 0, \quad j = 1, \dots, s.$$

According to [18, 17], the necessary and sufficient condition for (2.2) to have stage order q is:

$$\frac{\mathbf{c}^\nu}{\nu!} - \frac{(-1)^\nu}{\nu!} \mathbf{u} - \frac{\mathbf{A}\mathbf{c}^{\nu-1}}{(\nu-1)!} - \frac{\mathbf{B}(\mathbf{c} - \mathbf{e})^{\nu-1}}{(\nu-1)!} = 0, \quad \nu = 1, \dots, q, \quad (2.4)$$

where $\mathbf{e} = [1, \dots, 1]^T \in \mathbb{R}^s$ and the power operator is applied component-wise. Note that the stage consistency condition ($\nu = 1$) determines the value of the abscissa vector,

$$\mathbf{c} = (\mathbf{A} + \mathbf{B}) \mathbf{e} - \mathbf{u}. \quad (2.5)$$

The TSRK method (2.2) has *order* p [17, 18] if the final approximation y_{n_F} to the solution $y(t_F)$ is of (global) order p , that is

$$y_{n_F} = y(t_F) + \mathcal{O}(h^p), \quad h \rightarrow 0.$$

Consider a TSRK method (2.2) with stage order $q \geq p - 1$. If the coefficients satisfy the additional conditions

$$\frac{1}{\nu!} - \frac{(-1)^\nu}{\nu!} \vartheta - \frac{\mathbf{v}^T \mathbf{c}^{\nu-1}}{(\nu-1)!} - \frac{\mathbf{w}^T (\mathbf{c} - \mathbf{e})^{\nu-1}}{(\nu-1)!} = 0, \quad \nu = 1, \dots, p, \quad (2.6)$$

then the method has order p [18, 17].

2.2. Partitioned TSRK methods. We consider the partitioned system of ODEs

$$y' = \begin{bmatrix} y_{\{1\}} \\ \vdots \\ y_{\{N\}} \end{bmatrix}' = \begin{bmatrix} f_{\{1\}}(y) \\ \vdots \\ f_{\{N\}}(y) \end{bmatrix} = \sum_{k=1}^N \begin{bmatrix} \mathbf{0} \\ f_{\{k\}}(y) \\ \mathbf{0} \end{bmatrix} = f(y) \quad (2.7)$$

with scalar quantities $y_{\{1\}}, \dots, y_{\{N\}}$. The ideas presented in this section, as well as the mathematical proofs, hold equally well for systems (2.7) partitioned in subvectors. Since the subvector partitioning complicates the notation without bringing any additional insight, we consider the case (2.7) where all components are scalar.

Each of the N ODEs for $y'_{\{k\}}$ is integrated using a different TSRK method

$$\frac{\mathbf{u}^{\{k\}}}{\vartheta^{\{k\}} \mid \left(\mathbf{v}^{\{k\}} \right)^T \mid \left(\mathbf{w}^{\{k\}} \right)^T}, \quad k = 1, \dots, N. \quad (2.8)$$

The coefficients of the methods (2.8) have to be coordinated such that the overall discretization of (2.7) has the desired accuracy and stability.

We focus on families of methods (2.8) that have several particular characteristics which make them suitable for the integration of PDEs, discretized in the method of lines.

Preservation of linear invariants. Preservation of linear invariants is an essential property for the integration of conservation laws [5, 6, 27]. For example, the numerical solution of the advection equation conserves the total mass of the system (to roundoff accuracy) if the space discretization is flux conservative, and the time discretization preserves linear invariants.

The family of TSRK methods(2.8) conserves linear invariants of the system if all the weights are equal to each other. Therefore of particular interest are methods which share the same theta

$$\vartheta^{\{k\}} = \vartheta, \quad k = 1, \dots, N, \quad (2.9)$$

and the same weight vectors

$$\mathbf{v}^{\{k\}} = \mathbf{v}, \quad \mathbf{w}^{\{k\}} = \mathbf{w}. \quad k = 1, \dots, N. \quad (2.10)$$

To be specific, consider a linear invariant of the ODE system (2.7)

$$\sum_{k=1}^N \mu_{\{k\}} f_{\{k\}}(y) = 0, \quad \forall y \quad \Rightarrow \quad \sum_{k=1}^N \mu_{\{k\}} y_{\{k\}}(t) = C = \text{constant}, \quad \forall t.$$

Assume that all the previous numerical solutions preserve this invariant

$$\sum_{k=1}^N \mu_{\{k\}} y_{\{k\},\ell} = C, \quad \ell = 0, \dots, n-1.$$

We want the method (2.2) to produce a next step solution y_n that also preserves the invariant. From (2.2b), (2.9), and (2.10) it follows that

$$\begin{aligned} \sum_{k=1}^N \mu_{\{k\}} y_{\{k\},n} &= (1 - \vartheta) \sum_{k=1}^N \mu_{\{k\}} y_{\{k\},n-1} + \vartheta \sum_{k=1}^N \mu_{\{k\}} y_{\{k\},n-2} \\ &\quad + h \sum_{j=1}^s v_j \sum_{k=1}^N \mu_{\{k\}} f_{\{k\}} \left(Y_{\{1\},j}^{[n]}, \dots, Y_{\{N\},j}^{[n]} \right) \\ &\quad + h \sum_{j=1}^s w_j \sum_{k=1}^N \mu_{\{k\}} f_{\{k\}} \left(Y_{\{1\},j}^{[n-1]}, \dots, Y_{\{N\},j}^{[n-1]} \right) \\ &= C. \end{aligned}$$

Note that due to the theta consistency (2.9) and linear conservation condition (2.10) the summations in j and k commute, and the linear invariant condition holds for the next step solution as well.

Internal consistency. We consider the case where that all individual methods (2.8) are stage consistent (2.5). Each method (2.8) computes stage values $Y_{\{k\}}^{[n]}$ that approximate the exact solution components $y_{\{k\}}(t_n + \mathbf{c}^{\{k\}} h)$ at abscissas $\mathbf{c}^{\{k\}} = (\mathbf{A}^{\{k\}} + \mathbf{B}^{\{k\}}) \mathbf{e} - \mathbf{u}^{\{k\}}$. For internal consistency it is desirable that the stage vectors $Y_{\{k\},i}^{[n]}$ for all components k approximate the exact solution at the same time moment, $t_n + c_i h$, for all k . Consequently, we focus on stage consistent methods which satisfy the simplifying assumption

$$\mathbf{u}^{\{k\}} = \mathbf{u}, \quad k = 1, \dots, N, \quad (2.11)$$

and for which the abscissae of all N TSRK methods are equal

$$\left(\mathbf{A}^{\{k\}} + \mathbf{B}^{\{k\}}\right) \cdot \mathbf{e} = \mathbf{c} + \mathbf{u}, \quad k = 1, \dots, N. \quad (2.12)$$

The class of methods under consideration. The class of partitioned TSRK methods under consideration enjoys the properties of theta-consistency (2.9), u-consistency (2.11) linear conservation (2.10), and stage consistency (2.12). This class is characterized by the tableaux

$$\frac{\mathbf{u}}{\vartheta} \left| \begin{array}{c|c} \mathbf{A}^{\{k\}} & \mathbf{B}^{\{k\}} \\ \mathbf{v}^T & \mathbf{w}^T \end{array} \right., \quad k = 1, \dots, N. \quad (2.13)$$

Partitioned methods in this family are written explicitly as follows:

$$Y_{\{k\},i}^{[n]} = (1 - \mathbf{u}_i) y_{\{k\},n-1} + \mathbf{u}_i y_{\{k\},n-2} \quad (2.14a)$$

$$+ h \sum_{j=1}^s a_{i,j}^{\{k\}} f_{\{k\}} \left(Y_{\{1\},j}^{[n]}, \dots, Y_{\{N\},j}^{[n]} \right) \\ + h \sum_{j=1}^s b_{i,j}^{\{k\}} f_{\{k\}} \left(Y_{\{1\},j}^{[n-1]}, \dots, Y_{\{N\},j}^{[n-1]} \right)$$

$$y_{\{k\},n} = (1 - \vartheta) y_{\{k\},n-1} + \vartheta y_{\{k\},n-2} \quad (2.14b)$$

$$+ h \sum_{j=1}^s v_j f_{\{k\}} \left(Y_{\{1\},j}^{[n]}, \dots, Y_{\{N\},j}^{[n]} \right) \\ + h \sum_{j=1}^s w_j f_{\{k\}} \left(Y_{\{1\},j}^{[n-1]}, \dots, Y_{\{N\},j}^{[n-1]} \right)$$

$$k = 1, \dots, N.$$

Note that each f and g function call in (2.14) uses the arguments $\left(Y_{\{1\},j}^{[\ell]}, \dots, Y_{\{N\},j}^{[\ell]} \right)$ with $\ell = n - 1$ or $\ell = n$. Due to the stage consistency property (2.12), all intermediate vectors approximate the solution at the same time, $Y_{\{i\},j}^{[\ell]} \approx y_{\{i\}}(t_\ell + c_j h)$, and therefore the entire argument vector is a consistent approximation of the solution $y(t_\ell + c_j h)$.

2.3. Order conditions for partitioned TSRK methods. The main theorem below discusses the order conditions for our class of partitioned TSRK (PTRK) methods.

THEOREM 2.1. *Consider the class (2.13) of partitioned TSRK methods which satisfy the internal stage consistency condition (2.12). If*

- *each individual method is zero stable,*
- *the starting values are of order p ,*
- *each individual method is of order p ,*
- *each individual method has stage order $q \geq p - 1$,*

then the numerical solution converges with order p ,

$$y_n - y(t_n) = \mathcal{O}(h^p), \quad \forall n.$$

We note that no additional “coupling” conditions are needed.

Proof. Following the approach of [17, 18] we define

$$\mathcal{A} = \bar{\mathcal{A}} \otimes \mathbf{I}_N = \begin{bmatrix} \mathbf{0} & \mathbf{I}_s & \mathbf{0} & \mathbf{0} \\ \mathbf{0} & \mathbf{0} & \mathbf{u} & \mathbf{e} - \mathbf{u} \\ \mathbf{0} & \mathbf{0} & 0 & 1 \\ \mathbf{0} & \mathbf{0} & \vartheta & 1 - \vartheta \end{bmatrix} \otimes \mathbf{I}_N, \quad \mathcal{B} = \begin{bmatrix} \mathbf{0} & \mathbf{0} & \mathbf{0} & \mathbf{0} \\ \mathbb{B} & \mathbb{A} & \mathbf{0} & \mathbf{0} \\ \mathbf{0} & \mathbf{0} & 0 & 0 \\ \mathbf{w} & \mathbf{v} & 0 & 0 \end{bmatrix}, \quad (2.15)$$

with \mathbf{I}_N being the N -dimensional identity matrix, $\mathbf{e} = [1, \dots, 1]^T$,

$$\mathbf{v} = \mathbf{v}^T \otimes \mathbf{I}_N, \quad \mathbf{w} = \mathbf{w}^T \otimes \mathbf{I}_N, \quad (2.16)$$

and

$$\mathbb{A} = \begin{bmatrix} \mathbf{A}^{\{1\}} & & \mathbf{0} \\ & \ddots & \\ \mathbf{0} & & \mathbf{A}^{\{N\}} \end{bmatrix}, \quad \mathbb{B} = \begin{bmatrix} \mathbf{B}^{\{1\}} & & \mathbf{0} \\ & \ddots & \\ \mathbf{0} & & \mathbf{B}^{\{N\}} \end{bmatrix}. \quad (2.17)$$

We also define the vectors

$$Y^{[n]} = \begin{bmatrix} Y_{\{1\}}^{[n]} \\ \vdots \\ Y_{\{N\}}^{[n]} \end{bmatrix}, \quad F(Y^{[n]}) = \begin{bmatrix} F_{\{1\}}(Y_{\{1\}}^{[n]}, \dots, Y_{\{N\}}^{[n]}) \\ \vdots \\ F_{\{N\}}(Y_{\{1\}}^{[n]}, \dots, Y_{\{N\}}^{[n]}) \end{bmatrix},$$

$$Y_{\{k\}}^{[n]} = \begin{bmatrix} Y_{\{k\},1}^{[n]} \\ \vdots \\ Y_{\{k\},s}^{[n]} \end{bmatrix}, \quad F_{\{k\}}(Y_{\{1\}}^{[n]}, \dots, Y_{\{N\}}^{[n]}) = \begin{bmatrix} f_{\{k\}}(Y_{\{1\},1}^{[n]}, \dots, Y_{\{N\},1}^{[n]}) \\ \vdots \\ f_{\{k\}}(Y_{\{1\},s}^{[n]}, \dots, Y_{\{N\},s}^{[n]}) \end{bmatrix},$$

for $k = 1, \dots, N$, and

$$Z_1 = \begin{bmatrix} \mathbf{0} \\ Y^{[1]} \\ y_0 \\ y_1 \end{bmatrix}, \quad Z_n = \begin{bmatrix} Y^{[n-1]} \\ Y^{[n]} \\ y_{n-1} \\ y_n \end{bmatrix}; \quad n \geq 2, \quad F(Z_n) = \begin{bmatrix} F(Y^{[n-1]}) \\ F(Y^{[n]}) \\ f(y_{n-1}) \\ f(y_n) \end{bmatrix}.$$

The PTSRK method (2.14) can be written as an A-method [17]

$$Z_n = \mathcal{A} Z_{n-1} + h \mathcal{B} F(Z_n). \quad (2.18)$$

Similarly, the following vector notations are used for the exact solution

$$y_{\{k\}}(t_{n-1} + \mathbf{c}h) = \begin{bmatrix} y_{\{k\}}(t_{n-1} + c_1 h) \\ \vdots \\ y_{\{k\}}(t_{n-1} + c_s h) \end{bmatrix}, \quad y(t_{n-1} + \mathbf{c}h) = \begin{bmatrix} y_{\{1\}}(t_{n-1} + \mathbf{c}h) \\ \vdots \\ y_{\{N\}}(t_{n-1} + \mathbf{c}h) \end{bmatrix},$$

$$F_{\{k\}}(y(t_{n-1} + \mathbf{c}h)) = \begin{bmatrix} f_{\{k\}}(y(t_{n-1} + c_1 h)) \\ \vdots \\ f_{\{k\}}(y(t_{n-1} + c_s h)) \end{bmatrix},$$

$$F(y(t_{n-1} + \mathbf{c}h)) = \begin{bmatrix} F_{\{1\}}(y(t_{n-1} + \mathbf{c}h)) \\ \vdots \\ F_{\{N\}}(y(t_{n-1} + \mathbf{c}h)) \end{bmatrix},$$

as well as

$$z(t_1) = \begin{bmatrix} \mathbf{0} \\ y(t_0 + \mathbf{c}h) \\ y(t_0) \\ y(t_1) \end{bmatrix}, \quad z(t_n) = \begin{bmatrix} y(t_{n-2} + \mathbf{c}h) \\ y(t_{n-1} + \mathbf{c}h) \\ y(t_{n-1}) \\ y(t_n) \end{bmatrix}, \quad F(z(t_n)) = \begin{bmatrix} F(y(t_{n-2} + \mathbf{c}h)) \\ F(y(t_{n-1} + \mathbf{c}h)) \\ F(y(t_{n-1})) \\ F(y(t_n)) \end{bmatrix}.$$

The local discretization error $h\mathbf{d}(t_n)$ is the residual obtained when the numerical approximation Z_n is replaced by the exact solution $z(t_n)$ in (2.18)

$$z(t_n) = \mathcal{A}z(t_{n-1}) + h\mathcal{B}F(z(t_n)) + h\mathbf{d}(t_n). \quad (2.19)$$

We partition $h\mathbf{d}$ into stage residuals, and full step residuals, as follows:

$$h\mathbf{d}(t_n) = h \begin{bmatrix} \mathbf{d}_{\text{stage}}^{(1)}(t_n) \\ \mathbf{d}_{\text{stage}}^{(2)}(t_n) \\ \mathbf{d}_{\text{step}}^{(1)}(t_n) \\ \mathbf{d}_{\text{step}}^{(2)}(t_n) \end{bmatrix}.$$

Each residual has components for each of the two steps used by the TSRK method, $\mathbf{d}_{\text{stage}}^{(\tau)} \in \mathbb{R}^{(s \cdot N)}$ and $\mathbf{d}_{\text{step}}^{(\tau)} \in \mathbb{R}^N$ for $\tau = 1, 2$. Using (2.16), (2.17), (2.18), and (2.19), we arrive at the following expressions for the different components of the residual:

$$\begin{aligned} h\mathbf{d}_{\text{stage}}^{(1)}(t_n) &= y(t_{n-2} + \mathbf{c}h) - y(t_{n-2} + \mathbf{c}h) = \mathbf{0}, \\ h\mathbf{d}_{\text{stage}}^{(2)}(t_n) &= y(t_{n-1} + \mathbf{c}h) - (\mathbf{e} - \mathbf{u}) \otimes \mathbf{I}_N y(t_{n-1}) - \mathbf{u} \otimes \mathbf{I}_N y(t_{n-2}) \\ &\quad - h\mathbf{A}F(y(t_{n-1} + \mathbf{c}h)) - h\mathbf{B}F(y(t_{n-1} + (\mathbf{c} - \mathbf{e})h)), \\ h\mathbf{d}_{\text{step}}^{(1)}(t_n) &= y(t_{n-1}) - y(t_{n-1}) = \mathbf{0}, \\ h\mathbf{d}_{\text{step}}^{(2)}(t_n) &= y(t_n) - (1 - \vartheta) y(t_{n-1}) - \vartheta y(t_{n-2}) \\ &\quad - h\mathbf{v}F(y(t_{n-1} + \mathbf{c}h)) - h\mathbf{w}F(y(t_{n-1} + (\mathbf{c} - \mathbf{e})h)). \end{aligned}$$

Expanding the above expressions in Taylor series about t_{n-1} leads to

$$\begin{aligned} h\mathbf{d}_{\text{stage}}^{(2)}(t_n) &= \begin{bmatrix} \sum_{\nu \geq 1} C_{\{1\}, \nu}^{\text{stage}} h^\nu y_{\{1\}}^{(\nu)}(t_{n-1}) \\ \vdots \\ \sum_{\nu \geq 1} C_{\{N\}, \nu}^{\text{stage}} h^\nu y_{\{N\}}^{(\nu)}(t_{n-1}) \end{bmatrix}, \\ h\mathbf{d}_{\text{step}}^{(2)}(t_n) &= \begin{bmatrix} \sum_{\nu \geq 1} C_\nu^{\text{step}} h^\nu y_{\{1\}}^{(\nu)}(t_{n-1}) \\ \vdots \\ \sum_{\nu \geq 1} C_\nu^{\text{step}} h^\nu y_{\{N\}}^{(\nu)}(t_{n-1}) \end{bmatrix}, \end{aligned}$$

where the coefficients $C_{\{k\}, \nu}^{\text{stage}}$ and C_ν^{step} are given by

$$C_{\{k\}, \nu}^{\text{stage}} = \frac{\mathbf{c}^\nu}{\nu!} - \frac{(-1)^\nu}{\nu!} \mathbf{u} - \frac{\mathbf{A}^{\{k\}} \mathbf{c}^{\nu-1}}{(\nu-1)!} - \frac{\mathbf{B}^{\{k\}} (\mathbf{c} - \mathbf{e})^{\nu-1}}{(\nu-1)!}, \quad (2.20)$$

$$C_\nu^{\text{step}} = \frac{1}{\nu!} - \frac{(-1)^\nu}{\nu!} \vartheta - \frac{\mathbf{v}^T \mathbf{c}^{\nu-1}}{(\nu-1)!} - \frac{\mathbf{w}^T (\mathbf{c} - \mathbf{e})^{\nu-1}}{(\nu-1)!}. \quad (2.21)$$

We note that the differentials $y_{\{k\}}^{(\nu)}$ can be expressed using the P-series formalism [13] to allow for a general analysis of order conditions. However, as we will require high stage order, there is no need for this in our case.

The global error in the solution after n_F steps is due to the accumulation of local discretization errors (2.19). To analyze the error propagation we subtract the discrete method (2.18) from its continuous analogue (2.19). This leads to the linear error recurrence relation

$$\mathbf{q}(t_n) = \mathcal{A}\mathbf{q}(t_{n-1}) + h\mathcal{B}\mathbf{r}(t_n) + h\mathbf{d}(t_n), \quad n = 2, \dots, n_F, \quad (2.22a)$$

$$\mathbf{q}(t_1) = \begin{bmatrix} \mathbf{q}_{\text{stage}}^{(1)}(t_1) \\ \mathbf{q}_{\text{stage}}^{(2)}(t_1) \\ \mathbf{q}_{\text{step}}^{(1)}(t_1) \\ \mathbf{q}_{\text{step}}^{(2)}(t_1) \end{bmatrix} = \begin{bmatrix} \mathbf{0} \\ y(t_0 + \mathbf{c}h) - Y^{[1]} \\ y(t_0) - y_0 \\ y(t_1) - y_1 \end{bmatrix}, \quad (2.22b)$$

where

$$\mathbf{q}(t_n) = \begin{bmatrix} \mathbf{q}_{\text{stage}}^{(1)}(t_n) \\ \mathbf{q}_{\text{stage}}^{(2)}(t_n) \\ \mathbf{q}_{\text{step}}^{(1)}(t_n) \\ \mathbf{q}_{\text{step}}^{(2)}(t_n) \end{bmatrix} = \begin{bmatrix} y(t_{n-2} + \mathbf{c}h) - Y^{[n-1]} \\ y(t_{n-1} + \mathbf{c}h) - Y^{[n]} \\ y(t_{n-1}) - y_{n-1} \\ y(t_n) - y_n \end{bmatrix}, \quad n \geq 2,$$

and

$$\mathbf{r}(t_n) = \begin{bmatrix} \mathbf{r}_{\text{stage}}^{(1)}(t_n) \\ \mathbf{r}_{\text{stage}}^{(2)}(t_n) \\ \mathbf{r}_{\text{step}}^{(1)}(t_n) \\ \mathbf{r}_{\text{step}}^{(2)}(t_n) \end{bmatrix} = \begin{bmatrix} F(y(t_{n-2} + \mathbf{c}h)) - F(Y^{[n-1]}) \\ F(y(t_{n-1} + \mathbf{c}h)) - F(Y^{[n]}) \\ F(y(t_{n-1})) - F(y_{n-1}) \\ F(y(t_n)) - F(y_n) \end{bmatrix}, \quad n \geq 2.$$

The solution to (2.22a) reads

$$\mathbf{q}(t_n) = \mathcal{A}^{n-1}\mathbf{q}(t_1) + h \sum_{\ell=1}^{n-1} \mathcal{A}^{n-1-\ell} \mathbf{d}(t_{\ell+1}) + h \sum_{\ell=1}^{n-1} \mathcal{A}^{n-1-\ell} \mathcal{B}\mathbf{r}(t_{\ell+1}). \quad (2.23)$$

It is shown in [18] that when the method (2.18) is zero-stable (i.e., when $-1 < \vartheta \leq 1$) the matrices \mathcal{A}^μ , $\mu \geq 2$, take the form

$$\mathcal{A}^\mu = \begin{bmatrix} \mathbf{0} & \mathbf{0} & \alpha_{1,1}^{(\mu)} & \alpha_{1,2}^{(\mu)} \\ \mathbf{0} & \mathbf{0} & \alpha_{2,1}^{(\mu)} & \alpha_{2,2}^{(\mu)} \\ \mathbf{0} & \mathbf{0} & \beta_{1,1}^{(\mu)} & \beta_{1,2}^{(\mu)} \\ \mathbf{0} & \mathbf{0} & \beta_{2,1}^{(\mu)} & \beta_{2,2}^{(\mu)} \end{bmatrix} \otimes \mathbf{I}_N,$$

with uniformly bounded $\alpha_{i,j}^{(\mu)}$ and $\beta_{i,j}^{(\mu)}$, $i, j = 1, 2$. Following the arguments presented in [17, Section 5.2] one obtains the global error of the method after n steps as

$$\begin{aligned} \mathbf{q}_{\text{step}}^{(2)}(t_n) &= h\mathbb{w}\mathbf{r}_{\text{stage}}^{(2)}(t_{n-1}) + h\mathbb{v}\mathbf{r}_{\text{stage}}^{(2)}(t_n) \\ &+ h(1 - \vartheta)\mathbb{v}\mathbf{r}_{\text{stage}}^{(2)}(t_{n-1}) + h(1 - \vartheta)\mathbb{w}\mathbf{r}_{\text{stage}}^{(2)}(t_{n-2}) \\ &+ h \sum_{\ell=1}^{n-3} \beta_{2,2}^{(n-1-\ell)} \left(\mathbb{w}\mathbf{r}_{\text{stage}}^{(2)}(t_\ell) + \mathbb{v}\mathbf{r}_{\text{stage}}^{(2)}(t_{\ell+1}) \right) + \mathcal{O}(h^p) \end{aligned} \quad (2.24)$$

under the assumptions that the starting values are approximations of order p , that is

$$\mathbf{q}_{\text{step}}^{(1)}(t_1) = \mathcal{O}(h^p), \quad \mathbf{q}_{\text{step}}^{(2)}(t_1) = \mathcal{O}(h^p)$$

and that the method has order of consistency p , that is

$$\mathbf{d}_{\text{step}}^{(2)}(t_l) = \mathcal{O}(h^p)$$

as $h \rightarrow 0$. The last assumption is equivalent to $C_\nu^{\text{step}} = 0, \nu = 1, \dots, p$. If we additionally assume that the stages of all N methods are of order $q \geq p - 1$, that is $C_{\{k\}, \nu}^{\text{stage}} = 0, \nu = 1, \dots, p - 1$, we obtain $\mathbf{q}_{\text{step}}^{(2)}(t_n) = \mathcal{O}(h^{q+1}) = \mathcal{O}(h^p), h \rightarrow 0$.

Summarizing, if the method is zero stable, the starting values are of order p , the local consistency error of the method is of order p and the stages of all TSRK schemes employed are at least of order $p - 1$, then the numerical solution converges with order p (i.e. $y_{n_F} - y(t_{n_F}) = \mathcal{O}(h^p)$). We want to note that no additional coupling conditions need to be satisfied in this case.

The result extends directly to systems of equations.

□

3. Implicit-explicit TSRK methods. We now consider IMEX TSRK methods, where the additive partitioning uses two parts ($N = 2$). We denote the method coefficients by

$$\mathbf{A}^{\{1\}} = \mathbf{A}, \quad \mathbf{A}^{\{2\}} = \widehat{\mathbf{A}}, \quad \mathbf{B}^{\{1\}} = \mathbf{B}, \quad \mathbf{B}^{\{2\}} = \widehat{\mathbf{B}},$$

where \mathbf{A}, \mathbf{B} describe an explicit TSRK method, while $\widehat{\mathbf{A}}, \widehat{\mathbf{B}}$ are the coefficients of an implicit TSRK method. Moreover, $\widehat{\mathbf{A}}$ is consider lower triangular, with $\widehat{\mathbf{A}}_{i,i} = \gamma$ for all stages $i = 1, \dots, s$.

The IMEX TSRK method reads:

$$Y_i^{[n]} = (1 - \mathbf{u}_i) y_{n-1} + \mathbf{u}_i y_{n-2} \tag{3.1a}$$

$$\begin{aligned} &+ h \sum_{j=1}^{i-1} a_{i,j} f(Y_j^{[n]}) + h \sum_{j=1}^s b_{i,j} f(Y_j^{[n-1]}) \\ &+ h \sum_{j=1}^{i-1} \widehat{a}_{i,j} g(Y_j^{[n]}) + h\gamma g(Y_i^{[n]}) + h \sum_{j=1}^s \widehat{b}_{i,j} g(Y_j^{[n-1]}), \end{aligned}$$

$$y_n = (1 - \vartheta) y_{n-1} + \vartheta y_{n-2} \tag{3.1b}$$

$$+ h \sum_{j=1}^s \left(v_j (f + g)(Y_j^{[n]}) + w_j (f + g)(Y_j^{[n-1]}) \right).$$

4. Stability aspects. For TSRK methods (2.3) the stability matrix takes the form

$$\mathbf{M}(z) = \begin{bmatrix} 1 - \vartheta + z\mathbf{v}^T \mathbf{S}(z)(\mathbf{e} - \mathbf{u}) & \vartheta + z\mathbf{v}^T \mathbf{S}(z)\mathbf{u} & \mathbf{w}^T + z\mathbf{v}^T \mathbf{S}(z)\mathbf{B} \\ 1 & 0 & \mathbf{0} \\ z\mathbf{S}(z)(\mathbf{e} - \mathbf{u}) & z\mathbf{S}(z)\mathbf{u} & z\mathbf{S}(z)\mathbf{B} \end{bmatrix}, \tag{4.1}$$

with $\mathbf{S}(z) = (\mathbf{I}_s - z\mathbf{A})^{-1}$ (see [17, p.95]). The method is linearly stable if the spectral radius of the stability matrix (4.1) is smaller than or equal to one. The stability region of the method is defined as

$$\mathcal{S} = \{z \in \mathbb{C} : \rho(M(z)) \leq 1\}.$$

4.1. Linear stability of the partitioned method. To assess the stability of the combined IMEX method, i.e., to see how the stability properties of the two methods combine when used in tandem, we apply the method to the linear scalar ODE

$$y' = \zeta y + \eta y, \quad \{ \text{where } f(y) = \zeta y, \quad g(y) = \eta y \}. \quad (4.2)$$

We denote the non-stiff and the stiff complex variables by $z = h\zeta$ and $x = h\eta$, respectively. The method (3.1) applied to the scalar test equation (4.2) gives

$$\begin{aligned} Y^{[n]} &= (\mathbf{e} - \mathbf{u}) y_{n-1} + \mathbf{u} y_{n-2} + (z \mathbf{A} + x \widehat{\mathbf{A}}) Y^{[n]} + (z \mathbf{B} + x \widehat{\mathbf{B}}) Y^{[n-1]} \\ y_n &= (1 - \vartheta) y_{n-1} + \vartheta y_{n-2} + (z + x) \mathbf{v}^T Y^{[n]} + (z + x) \mathbf{w}^T Y^{[n-1]}. \end{aligned}$$

Solving this equation leads to

$$\begin{bmatrix} y_n \\ y_{n-1} \\ Y^{[n]} \end{bmatrix} = \mathbf{M}(x, z) \cdot \begin{bmatrix} y_{n-1} \\ y_{n-2} \\ Y^{[n-1]} \end{bmatrix}$$

with

$$\mathbf{M}(x, z) = \begin{bmatrix} \mathbf{M}_{1,1}(x, z) & \mathbf{M}_{1,2}(x, z) & \mathbf{M}_{1,3}(x, z) \\ 1 & 0 & \mathbf{0}_{1 \times s} \\ \mathbf{S}(x, z) (\mathbf{e} - \mathbf{u}) & \mathbf{S}(x, z) \mathbf{u} & \mathbf{S}(x, z) (z \mathbf{B} + x \widehat{\mathbf{B}}) \end{bmatrix}, \quad (4.3)$$

where

$$\begin{aligned} \mathbf{S}(x, z) &= (\mathbf{I}_s - z \mathbf{A} - x \widehat{\mathbf{A}})^{-1}, \\ \mathbf{M}_{1,1}(x, z) &= (1 - \vartheta) + (z \mathbf{v} + x \widehat{\mathbf{v}})^T \mathbf{S}(x, z) (\mathbf{e} - \mathbf{u}), \\ \mathbf{M}_{1,2}(x, z) &= \vartheta + (z \mathbf{v} + x \widehat{\mathbf{v}})^T \mathbf{S}(x, z) \mathbf{u}, \\ \mathbf{M}_{1,3}(x, z) &= (z \mathbf{v} + x \widehat{\mathbf{v}})^T \mathbf{S}(x, z) (z \mathbf{B} + x \widehat{\mathbf{B}}) + z \mathbf{w}^T + x \widehat{\mathbf{w}}^T. \end{aligned}$$

Theoretical results about the spectral radius of the matrix (4.3) are difficult to obtain. Instead, the joint stability is analyzed numerically as follows. Define a desired stiff stability region $\mathcal{S} \subset \mathbb{C}$, for example $\mathcal{S}_\alpha = \{x \in \mathbb{C}^- : |\text{imag}(x)| \leq \tan(\alpha) |\text{real}(x)|\}$ for $A(\alpha)$ -stability, and compute numerically the corresponding non-stiff stability region:

$$\mathcal{N}_\alpha = \{z \in \mathbb{C} : \rho(\mathbf{M}(x, z)) \leq 1, \quad \forall x \in \mathcal{S}_\alpha\}. \quad (4.4)$$

If the non-stiff stability regions are not degenerate for \mathcal{S} corresponding to $A(\alpha)$ -stability, e.g., $\alpha \in \{45^\circ, 75^\circ, 90^\circ\}$, then the IMEX combined stability is considered acceptable.

4.2. Prothero-Robinson convergence. We now study the possible order reduction for very stiff systems. We consider the Prothero-Robinson (PR) [22] test problem written as a split system (1.1)

$$y' = \underbrace{\mu(y - \phi(t))}_{g(y)} + \underbrace{\phi'(t)}_{f(y)}, \quad \mu < 0, \quad y(0) = \phi(0), \quad (4.5)$$

where the exact solution is $y(t) = \phi(t)$. A numerical method is said to be PR-convergent with order p if its application to (4.5) gives a solution whose the global error decreases as $\mathcal{O}(h^p)$ for $h \rightarrow 0$ and $h\mu \rightarrow -\infty$.

THEOREM 4.1. *Consider the IMEX TSRK method (3.1) of order p , stage order q for the explicit part, and stage order \hat{q} for the implicit part. Assume that the implicit part is linearly stable, and that the spectral radius of the implicit stability matrix (4.3) is bounded uniformly in an infinite region of the complex plane*

$$\rho\left(\widehat{\mathbf{M}}(z)\right) \leq \rho_0 < 1, \quad \forall z : \text{real}(z) \leq z_0 < 0, \quad |\text{imag}(z)| \leq \alpha \text{real}(z), \quad \alpha \geq 0.$$

Then the IMEX method (3.1) is PR-convergent with order $\min(p, q)$.

In particular if the explicit stage order is $q = p$, then the PR order of convergence is p . It is convenient to construct IMEX TSRK methods (3.1) with explicit stage order $q = p$, even if $\hat{q} = p - 1$, as such methods do not suffer from order reduction on the PR problem.

Proof. Let

$$\phi^{[n]} = \phi(t_{n-1} + \mathbf{c}h) = [\phi(t_{n-1} + c_1 h), \dots, \phi(t_{n-1} + c_s h)]^T.$$

The method (3.1) applied to (4.5) reads:

$$Y^{[n]} = (\mathbf{e} - \mathbf{u}) y_{n-1} + \mathbf{u} y_{n-2} + h \mathbf{A} \phi'^{[n]} + h \mathbf{B} \phi'^{[n-1]} \quad (4.6a)$$

$$+ h \mu \widehat{\mathbf{A}} \left(Y^{[n]} - \phi^{[n]} \right) + h \mu \widehat{\mathbf{B}} \left(Y^{[n-1]} - \phi^{[n-1]} \right),$$

$$y_n = (1 - \vartheta) y_{n-1} + \vartheta y_{n-2} + h \mathbf{v}^T \phi'^{[n]} + h \mathbf{w}^T \phi'^{[n-1]} \quad (4.6b)$$

$$+ h \mu \mathbf{v}^T \left(Y^{[n]} - \phi^{[n]} \right) + h \mu \mathbf{w}^T \left(Y^{[n-1]} - \phi^{[n-1]} \right).$$

Consider the global errors

$$e_n = y_n - \phi(t_n), \quad E^{[n]} = Y^{[n]} - \phi^{[n]}.$$

Write the stage equation (4.6a) in terms of the exact solution and global errors

$$E^{[n]} = -\phi(t_{n-1} + \mathbf{c}h) + (\mathbf{e} - \mathbf{u}) \phi(t_{n-1}) + \mathbf{u} \phi(t_{n-2})$$

$$+ (\mathbf{e} - \mathbf{u}) e_{n-1} + \mathbf{u} e_{n-2}$$

$$+ h \mathbf{A} \phi'(t_{n-1} + \mathbf{c}h) + h \mathbf{B} \phi'(t_{n-2} + \mathbf{c}h)$$

$$+ h \mu \widehat{\mathbf{A}} E^{[n]} + h \mu \widehat{\mathbf{B}} E^{[n-1]},$$

to obtain

$$\left(\mathbf{I} - h \mu \widehat{\mathbf{A}} \right) E^{[n]} = (\mathbf{e} - \mathbf{u}) e_{n-1} + \mathbf{u} e_{n-2} + h \mu \widehat{\mathbf{B}} E^{[n-1]} \quad (4.7)$$

$$- (\phi(t_{n-1} + \mathbf{c}h) - \mathbf{e} \phi(t_{n-1})) + \mathbf{u} (\phi(t_{n-2}) - \phi(t_{n-1}))$$

$$+ h \mathbf{A} \phi'(t_{n-1} + \mathbf{c}h) + h \mathbf{B} \phi'(t_{n-2} + \mathbf{c}h).$$

The exact solution is expanded in Taylor series about t_{n-1} :

$$\begin{aligned}\phi(t_{n-1} + \mathbf{c}h) - \mathbf{e}\phi(t_{n-1}) &= \sum_{k=1}^{\infty} \frac{h^k \mathbf{c}^k}{k!} \phi^{(k)}(t_{n-1}), \\ \phi(t_{n-2}) - \phi(t_{n-1}) &= \sum_{k=1}^{\infty} \frac{(-1)^k h^k}{k!} \phi^{(k)}(t_{n-1}), \\ h\phi'(t_{n-1} + \mathbf{c}h) &= \sum_{k=1}^{\infty} \frac{kh^k \mathbf{c}^{k-1}}{k!} \phi^{(k)}(t_{n-1}), \\ h\phi'(t_{n-2} + \mathbf{c}h) &= \sum_{k=1}^{\infty} \frac{kh^k (\mathbf{c} - \mathbf{e})^{k-1}}{k!} \phi^{(k)}(t_{n-1}).\end{aligned}$$

Inserting the above Taylor expansions in (4.7) leads to

$$\begin{aligned}(\mathbf{I} - h\mu \widehat{\mathbf{A}}) E^{[n]} &= (\mathbf{e} - \mathbf{u}) e_{n-1} + \mathbf{u} e_{n-2} + h\mu \widehat{\mathbf{B}} E^{[n-1]} \\ &\quad + \sum_{k=1}^{\infty} (-\mathbf{c}^k + (-1)^k \mathbf{u} + k \mathbf{A} \mathbf{c}^{k-1} + k \mathbf{B} (\mathbf{e} - \mathbf{c})^{k-1}) \frac{h^k}{k!} \phi^{(k)}(t_{n-1}) \\ &= (\mathbf{e} - \mathbf{u}) e_{n-1} + \mathbf{u} e_{n-2} + h\mu \widehat{\mathbf{B}} E^{[n-1]} + \mathcal{O}(h^{q+1})\end{aligned}$$

where q is the stage order of the explicit method. The last equality follows from the stage order conditions (2.4). Let $z = h\mu$. We have:

$$\begin{aligned}E^{[n]} &= \widehat{\mathbf{S}}(z) (\mathbf{e} - \mathbf{u}) e_{n-1} + \widehat{\mathbf{S}}(z) \mathbf{u} e_{n-2} + z \widehat{\mathbf{S}}(z) \widehat{\mathbf{B}} E^{[n-1]} + \mathcal{O}(h^{q+1}), \quad (4.8) \\ \widehat{\mathbf{S}}(z) &= (\mathbf{I} - z \widehat{\mathbf{A}})^{-1}.\end{aligned}$$

From (4.8) it follows that

$$\begin{aligned}z \mathbf{v}^T E^{[n]} &= z \mathbf{v}^T \widehat{\mathbf{S}}(z) (\mathbf{e} - \mathbf{u}) e_{n-1} + z \mathbf{v}^T \widehat{\mathbf{S}}(z) \mathbf{u} e_{n-2} \\ &\quad + z^2 \mathbf{v}^T \widehat{\mathbf{S}}(z) \widehat{\mathbf{B}} E^{[n-1]} + \mathcal{O}(h^{q+1}).\end{aligned} \quad (4.9)$$

Note that h and $h\mu$ are allowed to vary independently, and therefore the order of the asymptotic term does not change upon multiplication by $z = h\mu$.

Similarly, write the solution equation (4.6b) in terms of the exact solution and global errors:

$$\begin{aligned}e_n &= -\phi(t_n) + (1 - \vartheta) \phi(t_{n-1}) + \vartheta \phi(t_{n-2}) \\ &\quad + (1 - \vartheta) e_{n-1} + \vartheta e_{n-2} \\ &\quad + h \mathbf{v}^T \phi'(t_{n-1} + \mathbf{c}h) + h \mathbf{w}^T \phi'(t_{n-2} + \mathbf{c}h) \\ &\quad + h\mu \mathbf{v}^T E^{[n]} + h\mu \mathbf{w}^T E^{[n-1]}.\end{aligned}$$

After rearranging the expression, and expanding the exact solution in Taylor series about t_{n-1} , we obtain

$$\begin{aligned}e_n &= (1 - \vartheta) e_{n-1} + \vartheta e_{n-2} + h\mu \mathbf{v}^T E^{[n]} + h\mu \mathbf{w}^T E^{[n-1]} \\ &\quad + \sum_{k=1}^{\infty} (-1 + (-1)^k \vartheta + k \mathbf{v}^T \mathbf{c}^{k-1} + k \mathbf{w}^T (\mathbf{c} - \mathbf{e})^{k-1}) \frac{h^k}{k!} \phi^{(k)}(t_{n-1}) \\ &= (1 - \vartheta) e_{n-1} + \vartheta e_{n-2} + h\mu \mathbf{v}^T E^{[n]} + h\mu \mathbf{w}^T E^{[n-1]} + \mathcal{O}(h^{p+1}). \quad (4.10)\end{aligned}$$

The last equality follows from the order conditions (2.6).

The following error recurrence is obtained by combining (4.8), (4.9), and (4.10)

$$\begin{bmatrix} e_n \\ e_{n-1} \\ E^{[n]} \end{bmatrix} = \widetilde{\mathbf{M}}(h\mu) \cdot \begin{bmatrix} e_{n-1} \\ e_{n-2} \\ E^{[n-1]} \end{bmatrix} + \mathcal{O}\left(h^{\min(p+1, q+1)}\right). \quad (4.11)$$

Assume a one-step, order p method is used to initialize both the step and the stage solutions of the TSRK method [17, Section 6.2]. The error starting values are $e_0 = 0$, $e_1 = \mathcal{O}(h^p)$, and $E^{[1]} = \mathcal{O}(h^p)$. The error amplification matrix

$$\widetilde{\mathbf{M}}(z) = \begin{bmatrix} 1 - \vartheta + z \mathbf{v}^T \widehat{\mathbf{S}}(z) (\mathbf{e} - \mathbf{u}) & \vartheta + z \mathbf{v}^T \widehat{\mathbf{S}}(z) \mathbf{u} & z (\mathbf{w}^T + z \mathbf{v}^T \widehat{\mathbf{S}}(z) \widehat{\mathbf{B}}) \\ 1 & 0 & 0 \\ \widehat{\mathbf{S}}(z) (\mathbf{e} - \mathbf{u}) & \widehat{\mathbf{S}}(z) \mathbf{u} & z \widehat{\mathbf{S}}(z) \widehat{\mathbf{B}} \end{bmatrix},$$

is similar to the the stability function (4.3) of the implicit method for any finite nonzero z , $\widetilde{\mathbf{M}}(z) \sim \widehat{\mathbf{M}}(z)$. Therefore its spectral radius is uniformly bounded below one for all $z = h\mu$ of interest. By standard numerical ODE arguments [13] the equation (4.11) implies convergence of global errors to zero at a rate $\|e_n\| = \mathcal{O}(h^{\min(p, q)})$. \square

5. Construction of practical IMEX TRSK methods. In this section we construct practical implicit-explicit TSRK schemes with order $p = s + 1$ and stage order $\widehat{q} = q = s$. The relatively large number of stages is necessary to be able to enforce the desired stability properties.

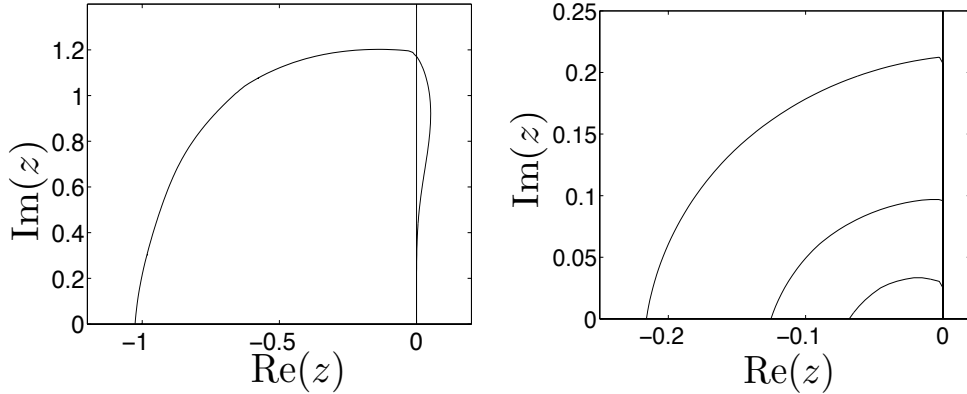
To construct an IMEX pair, we first choose an implicit TSRK method with appropriate stability properties (e.g., A or L -stability). The free parameters of the explicit method are the entries of the \mathbf{A} matrix. The coefficients \mathbf{B} of the nonstiff method result from the explicit stage order conditions (2.20) and the internal consistency conditions (2.12). The \mathbf{A} coefficients are computed using a numerical optimization procedure related to [23], with the aim to obtain an explicit stability region that contains the longest possible interval along the imaginary axis. An alternative strategy, not reported here, is to optimize for including the largest half ellipse with the semi-axis overlapping the imaginary axis. The optimization process is done in two steps. First, we explore the parameter space by means of a genetic algorithm [12]. The best member of this process is then taken as the starting point for the MATLAB `fminsearch` routine, which locally refines the solution and provides a sufficient number of accurate digits.

5.1. A fourth order, three stage IMEX pair. This method is characterized by $s = 3$, $p = 4$, and $q = 3$. The implicit part is taken from [1] and is L -stable. Our optimization yields the coefficients \mathbf{A} . All method coefficients \mathbf{c} , \mathbf{u} , \mathbf{B} , $\widehat{\mathbf{A}}$, $\widehat{\mathbf{B}}$, ϑ , \mathbf{v} , and \mathbf{w} are given in Appendix A for completeness.

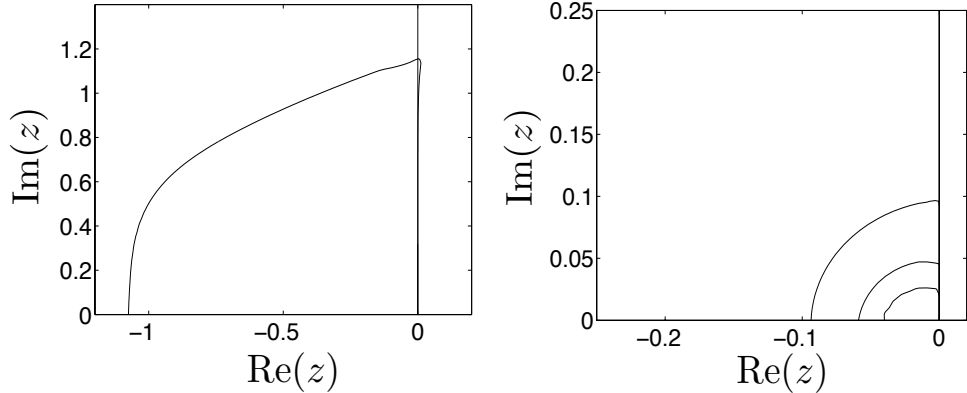
The region of stability for this explicit method is shown in Fig. 5.1(a),(b). The regions of combined stability for different choices of the stiff stability region \mathcal{S} are smaller than the unconstrained stability region, but are nontrivial and include a part of the imaginary axis.

5.2. A sixth order, five stage IMEX pair. This method is characterized by $s = 5$, $p = 6$, and $q = 5$. The implicit part is again taken from [1] and is L -stable. The coefficients \mathbf{A} are obtained by numerical optimization. All method coefficients \mathbf{c} , \mathbf{u} , \mathbf{B} , $\widehat{\mathbf{A}}$, $\widehat{\mathbf{B}}$, ϑ , \mathbf{v} , and \mathbf{w} are given in Appendix B for completeness.

The region of stability for this method is shown in Fig. 5.1(c),(d). Note that the regions of combined stability for different choices of the stiff stability region \mathcal{S} are smaller than the unconstrained stability region but are nontrivial and include a part of the imaginary axis.



(a) The fourth order method. Unconstrained explicit stability region. (b) The fourth order method. Constrained explicit stability regions \mathcal{N}_α for $\alpha \in \{45^\circ, 75^\circ, 90^\circ\}$.



(c) The sixth order method. Unconstrained explicit stability region. (d) The sixth order method. Constrained explicit stability regions \mathcal{N}_α for $\alpha \in \{45^\circ, 75^\circ, 90^\circ\}$.

FIG. 5.1. (a),(c) Stability regions for the explicit parts of the proposed IMEX-TSRK methods. (b),(d) The explicit stability regions \mathcal{N}_α in (4.4) are constrained by the $A(\alpha)$ stability of the implicit part. The explicit stability regions \mathcal{N}_α shown here correspond to $\alpha = 45^\circ$ (outer contours), $\alpha = 75^\circ$ (middle contours), and $\alpha = 90^\circ$ (inner contours).

6. Numerical tests. We now illustrate the convergence properties of the proposed IMEX TSRK schemes with the help of several test problems. For each of the test cases below a reference solution was computed with MATLAB's `ode15s` routine with the very tight tolerances $\text{atol} = \text{rtol} = 2.22045 \cdot 10^{-14}$. All numerical errors are measured at the final simulation times against the corresponding reference solutions.

6.1. Advection-reaction system. This test case is borrowed from [16] and is described by the following PDE system:

$$\partial_t \begin{bmatrix} y \\ z \end{bmatrix} = -\partial_x \begin{bmatrix} \alpha_1 y \\ \alpha_2 z \end{bmatrix} + \begin{bmatrix} -k_1 & k_2 \\ k_1 & -k_2 \end{bmatrix} \cdot \begin{bmatrix} y \\ z \end{bmatrix} + \begin{bmatrix} s_1 \\ s_2 \end{bmatrix}, \quad (t, x) \in [0, 1] \times [0, 1], \quad (6.1)$$

with parameters

$$\begin{bmatrix} \alpha_1 \\ \alpha_2 \end{bmatrix} = \begin{bmatrix} 1 \\ 0 \end{bmatrix}, \quad \begin{bmatrix} k_1 \\ k_2 \end{bmatrix} = 10^6 \cdot \begin{bmatrix} 1 \\ 2 \end{bmatrix}, \quad \begin{bmatrix} s_1 \\ s_2 \end{bmatrix} = \begin{bmatrix} 0 \\ 1 \end{bmatrix}, \quad (6.2)$$

and with the following initial and boundary values

$$y(x, 0) = 1 + s_2 x, \quad z(x, 0) = \frac{k_1}{k_2} y(x, 0) + \frac{1}{k_2} s_2, \quad y(0, t) = 1 - \sin(12t)^4. \quad (6.3)$$

The space discretization is done with fourth order finite differences in the interior and third order upwind biased finite differences at the borders of the spatial domain. The space grid consists of 400 uniformly distributed nodes. We treat the nonstiff advection term explicitly, and the stiff reaction term implicitly.

Several IMEX TSRK solutions are computed with different fixed time steps. They are compared against MATLAB's reference solution at the final time. The error maximum-norms are plotted against the time step in Fig. 6.1. We see that the solutions of both schemes display the theoretical convergence orders. Moreover, for equal time step sizes h , the sixth order scheme yields substantially smaller errors than the fourth order scheme. In summary, for the linear advection reaction test, both IMEX schemes behave as predicted by theory.

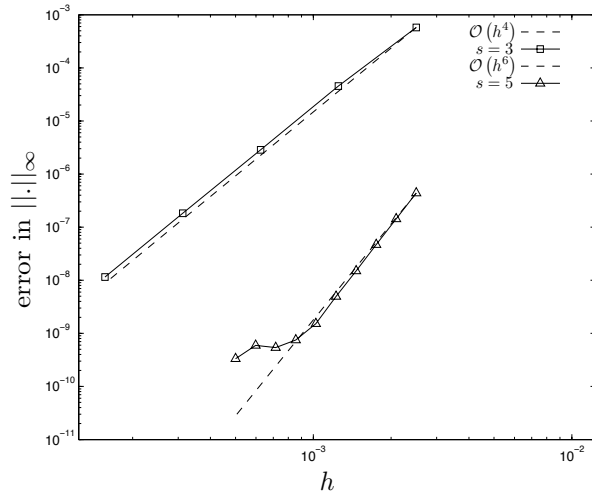


FIG. 6.1. Convergence of the proposed IMEX-TSRK schemes ($s = 3$ and $s = 5$) for the advection-diffusion test case. The solution errors (measured at the final time in maximum norm) are plotted against the simulation time step h .

6.2. Van der Pol equation. The first non-linear test is the van der Pol equation

$$\frac{d}{dt} \begin{bmatrix} y \\ z \end{bmatrix} = f(y, z) + g(y, z) = \begin{bmatrix} z \\ 0 \end{bmatrix} + \begin{bmatrix} 0 \\ ((1 - y^2)z - y)/\epsilon \end{bmatrix}, \quad 0 \leq t \leq 0.55139, \quad (6.4)$$

with parameter values taken from [2]

$$\epsilon = 10^{-5}, \quad y(0) = 2, \quad z(0) = -\frac{2}{3} + \frac{10}{81}\epsilon - \frac{292}{2187}\epsilon^2 - \frac{1814}{19683}\epsilon^3 + \mathcal{O}(\epsilon^4). \quad (6.5)$$

We integrate equation (6.4) with the IMEX TSRK methods with different fixed step sizes. The results at the final time are compared against the MATLAB reference solution. The errors in maximum-norm are plotted against step sizes in Fig. 6.2. The $p = 4$ scheme displays a convergence order close to four. The $p = 6$ scheme displays an effective order of 5.41. This result is in agreement with the order reduction predicted by Theorem 4.1, since the stage order of the explicit part is $q = 5$. In general both schemes show satisfactory convergence behavior.

For comparison purposes we consider the IMEX Additive Runge-Kutta (ARK) scheme [19] with $s = 8$ stages and order $p = 5$. The results are shown in Fig. 6.3. While in the non-stiff case ($\epsilon = 10^{-1}$) the scheme displays the expected fifth order, in the stiff case ($\epsilon = 10^{-5}$) the effective order of the scheme is one. The IMEX ARK method uses more right hand side evaluations per step (eight) than the IMEX TSRK methods (three and five, respectively), and also suffers from severe order reduction. This test case illustrates the benefit of the proposed IMEX TSRK schemes.

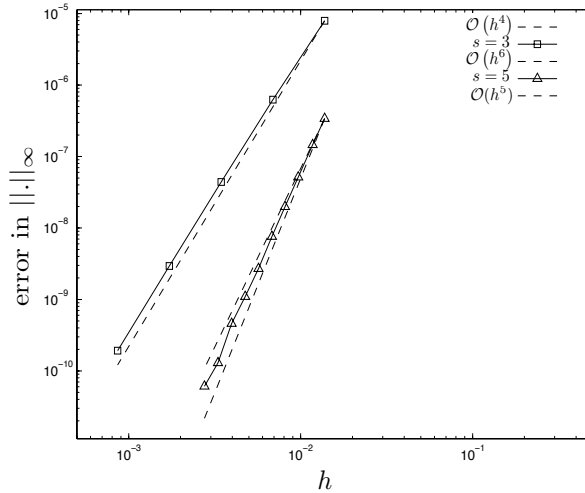


FIG. 6.2. Convergence of the proposed IMEX-TSRK schemes for the stiff van der Pol equation 6.4 with $\epsilon = 10^{-5}$. The solution errors (measured at the final time in maximum norm) are plotted against the simulation time step h .

6.3. Shallow water equations. *Semi-implicit time integration* has become popular in the numerical weather and climate prediction communities, e.g., as an effective way to treat gravity waves. Semi-implicit integration uses an IMEX scheme, with the implicit method applied to the linearized right hand side operator, and the explicit method to the remaining nonlinear part. This approach goes back to [25].

In this test we solve the two dimensional shallow water equations using a semi-implicit integration approach. The discretization is based on the proposed IMEX

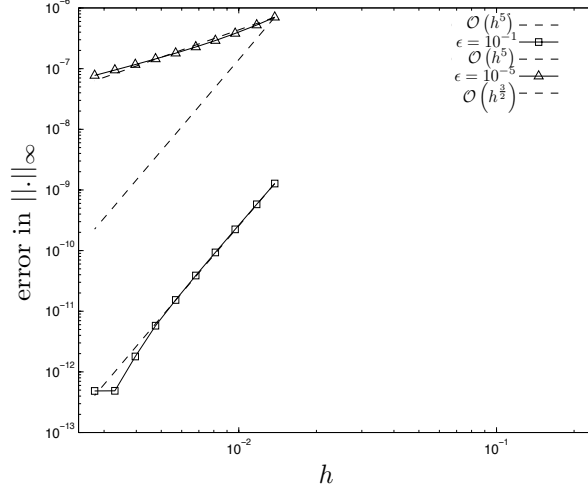


FIG. 6.3. Convergence of the ARK scheme for the van der Pol equation 6.4. In case non-stiff case ($\epsilon = 10^{-1}$) the integrator shows the expected order five behavior. However in the stiff case ($\epsilon = 10^{-5}$) the integrator shows order reduction with an effective order of about 1.5. The solution errors (measured at the final time in maximum norm) are plotted against the simulation time step h .

TSRK methods. The shallow water system under consideration is

$$\begin{aligned}\partial_t H &= -\partial_x(uH) - \partial_y(vH) \\ \partial_t(uH) &= -\partial_x(u^2H + \frac{1}{2}gH^2) - \partial_y(uvH) \\ \partial_t(vH) &= -\partial_x(uvH) - \partial_y(v^2H + \frac{1}{2}gH^2)\end{aligned}\tag{6.6}$$

on the unit square domain $(x, y) \in [0, 1] \times [0, 1]$. Here H is the fluid height, and u and v are the flow velocity components. The initial conditions at $t_0 = 0$ are

$$u(t_0, x, y) = 0, \quad v(t_0, x, y) = 0, \quad H(t_0, x, y) = 1 + \exp(-\|(x, y) - (c_1, c_2)\|_2^2), \tag{6.7}$$

where the Gaussian height profile is described by $c_1 = 1/3$ and $c_2 = 2/3$. Furthermore, the local gravity constant is $g = 9.81 [m/sec^2]$. Reflective boundary conditions are used. The initial condition produces traveling waves that suffer multiple reflections at the boundaries.

This test follows the shallow water example in [20]. A second order finite difference scheme is used for space discretization. The resulting semi-discrete ODE system is

$$\frac{d}{dt}U(t) = F_{\text{swe}}(U(t)), \tag{6.8}$$

where $U(t)$ is the discrete counterpart of the vector of unknowns (H, Hu, Hv) . Let $J_{\text{swe}} = dF_{\text{swe}}/dU$ be the Jacobian of the discretized shallow water operator. We split the right hand side of equation (6.8) into a stiff part

$$g(U(t)) = J_{\text{swe}}(U(t)) \cdot U(t), \tag{6.9}$$

and a non-stiff part

$$f(U(t)) = F_{\text{swe}}(U(t)) - g(U(t)). \tag{6.10}$$

Here g is a non-linear function in $U(t)$. The numerical solution of the implicit part of the method uses a simplified Newton iteration that requires only a single factorization of $\mathbf{I} - h\lambda J_{swe}(U_n)$ per step. Here U_n is the numerical approximation to $U(t_n)$. Note that a semi-implicit approach can be obtained similarly by choosing a linear stiff part, i.e., a splitting of the form $g(U) = J_{swe}(U_n) \cdot (U(t) - U_n)$ on each step $t \in [t_n, t_{n+1}]$.

We integrate the system from $t_0 = 0$ to $t_F = 10$ [seconds]. The final time solutions obtained with the IMEX TSRK schemes are compared against the Matlab reference solution. The error max-norms are plotted against the time step size in Fig. 6.4. Both schemes behave as expected, and display the theoretical orders of convergence.

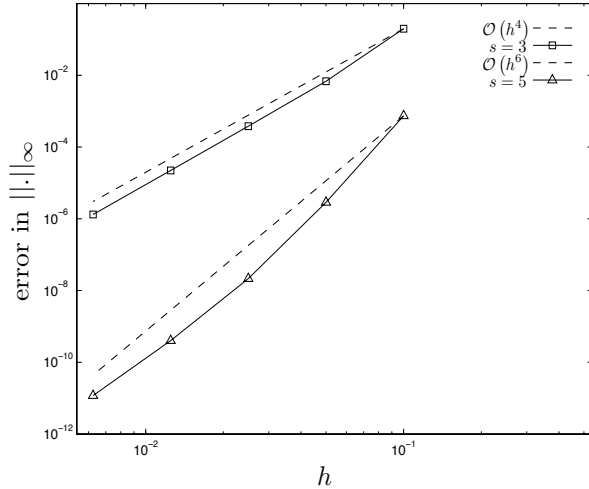


FIG. 6.4. Convergence of the proposed IMEX-TSRK schemes for the shallow water equations. The solution errors (measured at the final time in maximum norm) are plotted against the simulation time step h .

7. Conclusions. This paper develops a new family of implicit-explicit time integrators based on pairs of two-step Runge-Kutta methods. The class of schemes of interest is characterized by stage consistency (same abscissae) and linear invariant preservation (same weights). The study of order conditions for partitioned TSRK methods reveals that, in case of high stage orders, no additional coupling conditions need to be satisfied. Therefore this framework offers extreme flexibility in pairing implicit and explicit methods. We construct two practical IMEX TSRK methods, of orders four and six, respectively. In both cases the implicit parts are L-stable and taken from the literature. The corresponding explicit parts have been constructed such as to maximize their stability properties; their coefficients were found via a numerical optimization approach. A convergence analysis for the Prothero-Robinson problem shows that the effective order of IMEX schemes in case of stiffness equals the stage order of the explicit part; a slight order reduction (from p to $q = p - 1$) is expected in the general case, but can be avoided in principle by using explicit methods with $q = p$.

Numerical examples include an advection diffusion system, the Van der Pol equation, and a semi-implicit integration of shallow water equations. On all tests the methods perform as predicted by the theory. In particular, the proposed schemes perform much better on the van der Pol test than an existing IMEX Runge Kutta method; the latter suffers from severe order reduction.

The new framework allows to obtain IMEX schemes of order p and stage order $p-1$ using only $s = p-1$ stages. For $p \geq 4$ this is an advantage over existing IMEX Runge-Kutta schemes. The proposed framework offers extreme flexibility in the construction of new partitioned methods, since no coupling conditions are necessary. This approach has the potential to increase the computational efficiency of multiphysics simulations where different physical phenomena need different numerical treatments.

REFERENCES

- [1] Z. Bartoszewski and Z. Jackiewicz. Construction of two-step Runge-Kutta methods of high order for ordinary differential equations. *Numer. Algorithms*, 18:51–70, 1998.
- [2] S. Boscarino. Error analysis of IMEX Runge-Kutta methods derived from differential-algebraic systems. *SIAM J. Numerical Analysis*, 45(4):1600–1621, 2007.
- [3] K. Burrage and J.C. Butcher. Non-linear stability of a general class of differential equation methods. *BIT*, 20(2):185–203, 1980.
- [4] J.C. Butcher. On the convergence of numerical solutions to ordinary differential equations. *Mathematics of Computation*, 20(93):1–10, jan 1966.
- [5] E.M. Constantinescu and A. Sandu. Multirate timestepping methods for hyperbolic conservation laws. *Journal on Scientific Computing*, 33(3):239–278, 2007.
- [6] E.M. Constantinescu and A. Sandu. Optimal explicit strong stability preserving general linear methods. *SIAM Journal on Scientific Computing*, 32(5):3130–3150, 2010.
- [7] G.J. Cooper. The order of convergence of general linear methods for ordinary differential equations. *SIAM Journal on Numerical Analysis*, 15(4):643–661, 1978.
- [8] V. Dolejsi, M. Feistauer, and J. Hozman. Analysis of semi-implicit dgfm for nonlinear convection-diffusion problems on nonconforming meshes. *Computer Methods in Applied Mechanics and Engineering*, 196:2813–2827, 2007.
- [9] J. Frank, W. Hundsdorfer, and J.G. Verwer. On the stability of imex lm methods. *Applied Numerical Mathematics*, 25:193–205, 1997.
- [10] L. Gebhardt, D. Fokin, Th. Lutz, and S. Wagner. An implicit-explicit Dirichlet-based field panel method for transonic aircraft design. AIAA Applied Aerodynamics Conference, June 2002.
- [11] F. Giraldo. Hybrid Eulerian-Lagrangian semi-implicit time-integrators. *International Journal of Computers and Mathematics with Applications*, 52:1325–1342, 2006.
- [12] M. B. Gordy. Genetic Algorithm Minimizer version 3.1 for MATLAB. <http://mgordy.tripod.com/research.html#software>.
- [13] E. Hairer, S.P. Norsett, and G. Wanner. *Solving ordinary differential equations I: Nonstiff problems*. Springer, 1993.
- [14] E. Hairer, S.P. Norsett, and G. Wanner. *Solving ordinary differential equations II: Stiff and differential-algebraic problems*. Springer, 1993.
- [15] E. Hairer and G. Wanner. Multistep-multistage-multiderivative methods for ordinary differential equations. *Computing*, 11(3):287–303, 1973.
- [16] W. Hundsdorfer and S.J. Ruuth. IMEX extensions of linear multistep methods with general monotonicity and boundedness properties. *Journal of Computational Physics*, 225:2016–2042, 2007.
- [17] Z. Jackiewicz. *General Linear Methods for Ordinary Differential Equations*. Wiley, Hoboken, New Jersey, 2009.
- [18] Z. Jackiewicz and S. Tracogna. A general class of two-step Runge-Kutta methods for ordinary differential equations. *SIAM J. Numer. Anal.*, 32(5):1390–1427, 1995.
- [19] A. C. Kennedy and M. H. Carpenter. Additive Runge-Kutta schemes for convection-diffusion-reaction equations. *Appl. Numer. Math.*, 44(1-2):139–181, 2003.
- [20] Cleve Moller. *Experiments with Matlab*. MathWorks, 2011.
- [21] L. Pareschi and G. Russo. Implicit-explicit Runge-Kutta schemes for stiff systems of differential equations. In *Recent trends in numerical analysis*, pages 269–288. Nova Science Publishers, Inc., 2000.
- [22] A. Prothero and A. Robinson. On the stability and accuracy of one-step methods for solving stiff systems of ordinary differential equations. *Math. Comput.*, 28:145–162, 1974.
- [23] A. R. Renault. Two-step Runge-Kutta methods and hyperbolic partial differential equations. *Math. Comput.*, 55(192):563–579, 1990.
- [24] M. Restelli and F. Giraldo. A conservative semi-implicit discontinuous Galerkin method for the Navier-Stokes equations in nonhydrostatic mesoscale modeling. *SIAM Journal on Scientific Computing*, in press, 2009.

- [25] A. Robert. The integration of a spectral model of the atmosphere by the implicit method. *Proceedings of the WMO/IUGG Symposium on NWP, Tokyo*, Japan Meteorological Agency:VII.19–VII.24, 1969.
- [26] S.J. Ruuth. Implicit-explicit methods for reaction-diffusion problems in pattern formation. *Journal of Mathematical Biology*, 34:148–176, 1995.
- [27] A. Sandu and E.M. Constantinescu. Multirate Adams Methods for Hyperbolic Equations. *Journal of Scientific Computing*, 38(2):229–249, 2009.
- [28] R. Skeel. Analysis of fixed-stepsize methods. *SIAM Journal on Numerical Analysis*, 13(5):664–685, oct 1976.
- [29] L. Skvortsov. Explicit two-step runge-kutta methods. *Mathematical Models and Computer Simulations*, 2:222–231, 2010. 10.1134/S2070048210020092.
- [30] S. Tracogna. Implementation of two-step runge-kutta methods for ordinary differential equations. *Journal of Computational and Applied Mathematics*, 76:113–136, 1996.
- [31] S. Tracogna and B. Welfert. Two-step Runge-Kutta: theory and practice. *BIT Numerical Mathematics*, 40:775–799, 2000. 10.1023/A:1022352704635.
- [32] U.M. Ascher and S.J. Ruuth and B.T.R. Wetton. Implicit-explicit methods for time-dependent partial differential equations. *SIAM Journal on Numerical Analysis*, 32(3):797–823, 1995.
- [33] U.M. Ascher and S.J. Ruuth and R.J. Spiteri. Implicit-explicit Runge-Kutta methods for time-dependent partial differential equations. *Applied Numerical Mathematics*, 25:151–167, 1997.
- [34] J. G. Verwer and B. P. Sommeijer. An implicit-explicit Runge–Kutta–Chebyshev scheme for diffusion-reaction equations. *SIAM Journal on Scientific Computing*, 25(5):1824–1835, 2004.
- [35] J.G. Verwer, J.G. Blom, and W. Hundsdorfer. An implicit-explicit approach for atmospheric transport-chemistry problems. *Applied Numerical Mathematics*, 20:191–209, 1996.

Appendix A. Coefficients of the fourth order IMEX TSRK method.

$$\begin{aligned}
\mathbf{c} &= [-0.19320190561126 \quad -0.58689424506961 \quad 1.08752332811466]^T \\
\mathbf{u} &= [0.45705571481934 \quad 1.05195992030028 \quad 0.15144080311463]^T \\
\mathbf{A} &= \begin{bmatrix} 0 & 0 & 0 \\ 0.130476793083096 & 0 & 0 \\ 1.649241112842109 & 1.814778592781876 & 0 \end{bmatrix} \\
\mathbf{B} &= \begin{bmatrix} 0.39936246636454 & -0.16633596050061 & 0.03082730334415 \\ 0.51702376261274 & -0.18175387306707 & -0.00068100739809 \\ -5.84960861008881 & 3.22359516594067 & 0.40095792975345 \end{bmatrix} \\
\widehat{\mathbf{A}} &= \begin{bmatrix} 0.5 & 0 & 0 \\ 0.55515820921130 & 0.5 & 0 \\ -0.27897090290997 & 2.32682280748097 & 0.5 \end{bmatrix} \\
\widehat{\mathbf{B}} &= \begin{bmatrix} 0.01138595046334 & 0.04659103146040 & -0.29412317271565 \\ -0.48129318880262 & 0.30924798197004 & -0.41804732714804 \\ -2.38622282079758 & 0.99017411095761 & 0.08716093649826 \end{bmatrix} \\
\vartheta &= 0 \\
\mathbf{v} &= [-0.70240474564317 \quad 2.11852316846112 \quad 0.39319598421807]^T \\
\mathbf{w} &= [-2.07554769770216 \quad 0.84049470544433 \quad 0.42573858522182]^T
\end{aligned} \tag{A.1}$$

Appendix B. Coefficients of the sixth order IMEX TSRK method.

$$\begin{aligned}
 \mathbf{c} &= [-0.40455452705961 \quad -0.26488149320550 \quad 0.05730060498812 \quad 0.35370097422467 \quad 0.48881518147020]^T \\
 \mathbf{u} &= [0.0002157372318872 \quad 0.0001354655498456 \quad 0.0000469196256648 \quad 0.0000256681792066 \quad 0.0000230139042425]^T \\
 \mathbf{A} &= \begin{bmatrix} 0 & 0 & 0 & 0 & 0 \\ -0.411067755933170 & 0 & 0 & 0 & 0 \\ -2.184767292491065 & 0.988337848532673 & 0 & 0 & 0 \\ -1.933520824847556 & -0.039861058310592 & 0.757541697266156 & 0 & 0 \\ -0.605970379043349 & -1.561665570720364 & 1.243988457457954 & 0.094790995264783 & 0 \end{bmatrix} \\
 \mathbf{B} &= \begin{bmatrix} -1.28995988436797 & 3.01509152040882 & -4.63540469340360 & 7.43932768849976 & -4.93339342096474 \\ -1.07127144661267 & 2.48892090515797 & -3.73103986608896 & 5.53336809422864 & -3.07365595840746 \\ -0.24158168198390 & 0.58513684309224 & -0.97567738262348 & 1.29786646201535 & 0.58803272807197 \\ -0.67042428681047 & 1.66052413771998 & -2.85719727361944 & 4.08269477244835 & -0.64603052144256 \\ -1.51656343997187 & 3.67738907820218 & -5.98650039451221 & 8.41545308430861 & -3.27208363610734 \end{bmatrix} \\
 \hat{\mathbf{A}} &= \begin{bmatrix} 0.5 & 0 & 0 & 0 & 0 \\ -0.21971694115244 & 0.5 & 0 & 0 & 0 \\ 0.34677391973940 & -0.87844580948604 & 0.5 & 0 & 0 \\ 0.06601787269656 & -1.14976271542161 & -0.08264051407691 & 0.5 & 0 \\ -1.69420405359670 & 0.16618320114019 & -0.74229361529808 & 0.20048354140037 & 0.5 \end{bmatrix} \\
 \hat{\mathbf{B}} &= \begin{bmatrix} -1.42651400380231 & 3.34568800074286 & -5.21803000182508 & 8.75340345119152 & -6.35888623613472 \\ -1.85213037155704 & 4.34496259959515 & -6.76681774290671 & 11.10081457512045 & -7.37185814675508 \\ -4.26388543763339 & 9.73682010462664 & -13.73465558507126 & 18.29003094666633 & -9.93929061422790 \\ -10.19622755259608 & 22.71041154118940 & -29.47781369898124 & 33.88465664359473 & -15.90091493400099 \\ -16.69367618197397 & 36.82959193421020 & -46.44024346854481 & 51.34375399377619 & -22.98075715573894 \end{bmatrix} \\
 \vartheta &= 0 \\
 \mathbf{v} &= [1.38310762038221 \quad -1.20955981252655 \quad 0.11281066473162 \quad -1.91985715272309 \quad 2.64595762329489]^T \\
 \mathbf{w} &= [-4.70654020323220 \quad 10.88079796245341 \quad -15.26460646566261 \quad 18.34573036115907 \quad -9.26784059787675]^T
 \end{aligned} \tag{B.1}$$